Ion Transport and Structural Dynamics in Homologous Ammonium and Phosphonium-Based Room Temperature Ionic Liquids

Philip J. Griffin[1*], Adam P. Holt[2], Katsuhiko Tsunashima[3], Joshua R. Sangoro[4], Friedrich Kremer[5], and Alexei P. Sokolov[2,6,7]

[1]*Department of Materials Science and Engineering, University of Pennsylvania, Philadelphia, PA 19104, USA*

[2]*Department of Physics and Astronomy, University of Tennessee, Knoxville, TN 37996, USA*

[3]*Department of Materials Science, National Institute of Technology, Wakayama College, 77 Noshima, Nada-cho, Gobo, Wakayama 644-0023, Japan*

[4]*Department of Chemical and Biomolecular Engineering, University of Tennessee, Knoxville, TN 37996, USA*

[5]*Institute of Experimental Physics I, University of Leipzig, Linnestr. 5, 04103 Leipzig, Germany*

[6]*Department of Chemistry, University of Tennessee, Knoxville, TN 37996, USA*

[7]*Chemical Sciences Division, Oak Ridge National Lab, Oak Ridge, TN 37830, USA*

[*]Corresponding Author:

Philip J. Griffin (pgrif@seas.upenn.edu)

ABSTRACT

Charge transport and structural dynamics in a homologous pair of ammonium and phosphonium based room temperature ionic liquids (ILs) have been characterized over a wide temperature range using broadband dielectric spectroscopy and quasi-elastic light scattering spectroscopy. We have found that the ionic conductivity of the phosphonium based IL is significantly enhanced relative to the ammonium homolog, and this increase is primarily a result of a lower glass transition temperature and higher ion mobility. Additionally, these ILs exhibit pronounced secondary relaxations which are strongly influenced by the atomic identity of the cation charge center. While the secondary relaxation in the phosphonium IL has the expected Arrhenius temperature dependence characteristic of local beta relaxations, the corresponding relaxation process in the ammonium IL was found to exhibit a mildly non-Arrhenius temperature dependence in the measured temperature range—indicative of molecular cooperativity. These differences in both local and long-range molecular dynamics are a direct reflection of the subtly different inter-ionic interactions and mesoscale structures found in these homologous ILs.

INTRODUCTION

Quaternary aprotic room temperature ionic liquids (IL) have many advantageous physicochemical properties relative to their cyclic analogs, such as enhanced hydrophobicity and significantly wider electrochemical windows, which make them promising materials for use in electrochemical applications.[1, 2] The most common quaternary ILs are composed of ammonium cation cores with varying length alkyl side chains. These ILs, however, tend to have relatively high viscosities and low ionic conductivities at ambient temperature.[3] Not only can this be attributed to the relatively large molecular size of the cation,[2, 4] but it is also attributable to the presence of hydrophobically aggregated nanoscale domains which impede the mobility of conducting ions.[5, 6]

It has been shown that aprotic quaternary phosphonium ILs are promising alternatives to their quaternary ammonium analogs. Phosphonium ILs possess similar hydrophobicity and electrochemical windows as ammonium ILs, and additionally they exhibit significantly reduced viscosities, enhanced ionic conductivities, as well as higher thermal degradation temperatures.[7] Shirota *et al*. argued that phosphonium ionic liquids exhibit lower viscosity when compared to their ammonium homologs because the phosphonium cation has a larger volume, which effectively lowers the cation charge density and the electrostatic friction between counterions.[8] However, recent studies have indicated that the polarizability of the cation center atom also significantly influences the electrostatic friction between counterions.[9] Phosphorus is more electronically polarizable than nitrogen, and as a result, the positive charge of the phosphonium cation is more localized to the phosphorus core than in a homologous ammonium IL.[10] Since the phosphonium core is shielded by relatively charge-neutral alkyl groups which surround this core, weaker organization between the cation and anion charge centers may occur, which can correspondingly lower the electrostatic friction in phosphonium ILs.

In accordance with these studies, recent 2D-NMR experiments of Lee *et al*. have shown that the mesoscale organization of phosphonium ILs is significantly different from that of homologous ammonium ILs.[11] It was demonstrated in this work that the anions of octyltriethylammonium bis(trifluoromethylsulfonyl)imide [N2228][NTF_2] interact much more readily with the cation charge center, while the anions of the analogous phosphonium IL [P2228][NTF_2] interact with the octyl tail as well as with the phosphonium charge center. While these experimental and computational studies have definitively shown that unique and pronounced changes are occurring in the local structures of these ILs upon substitution of nitrogen with phosphorus, the corresponding impact of these differences on charge transport and structural dynamics are not yet well understood.

In this article, we present studies of the ion transport and structural dynamics in a homologous pair of ammonium and phosphonium based room temperature ionic liquids, [N2228][NTF_2] and [P2228][NTF_2], over a broad temperature range using broadband dielectric spectroscopy (BDS) and depolarized dynamic light scattering (DDLS). We have found that the ionic (dc) conductivity of the phosphonium IL is significantly higher than that of the corresponding ammonium IL at all measured temperatures. Increased ionic conductivity is attributed to the significantly lower calorimetric glass transition temperature and enhanced molecular mobility of [P2228][NTF_2] relative to [N2228][NTF_2]. We have also found that the atomic identity of the cation charge center strongly influences the secondary relaxations in these homologous ILs. Whereas the secondary relaxations in [P2228][NTF_2] exhibit the usual Arrhenius type of temperature dependence characteristic of β relaxations, the corresponding relaxation process in [N2228][NTF_2] exhibits weakly non-Arrhenius type of temperature dependence and is thus mildly cooperative in nature. We propose that this unusual finding and the contrasting local dynamics of

[N2228][NTF_2] and [P2228][NTF_2] are a direct result of the differences in the interionic interactions in these seemingly similar ILs.

EXPERIMENTAL SECTION

Octyltriethylammonium bis(trifluoromethylsulfonyl)imide ([N2228][NTF_2]) was obtained from Iolitec USA (M_w = 494.56 g/mol), and octyltriethylphosphonium bis(trifluoromethylsulfonyl)imide ([P2228][NTF_2]) was obtained from Nippon Chemical Industrial Co. (M_w = 511.52 g/mol). The chemical structures of these ILs are depicted in Fig. 1. Prior to measurement, the samples were filtered through 0.22 micron PVDF filters into cleaned, dried milliliter-sized glass vials. The filtered ILs were then placed in a vacuum oven at T = 75°C and P = 1 mbar for at least 24 h to remove residual solvents or dissolved gasses, after which they were quickly sealed under ambient conditions. The calorimetric glass transition temperature T_g of [N2228][NTF_2] (T_g = 193 ± 2 K) and [P2228][NTF_2] (T_g = 186 ± 2 K) was measured on cooling at a rate of 5 K/min using a Q1000 differential scanning calorimeter (TA instruments).

Broadband dielectric spectroscopy (BDS) was used to measure the ionic conductivity and dipolar relaxations in these ILs over temperatures ranging from 185–300 K. These measurements were performed using a Novocontrol Alpha-A dielectric analyzer in the frequency range 10^{-1} Hz to 10 MHz. The liquid samples were mounted between 15 mm diameter cylindrical stainless steel electrodes, using small Teflon spacer posts to maintain a sample thickness of 0.1 mm. The temperature of the sample was controlled using the Novocontrol Quatro temperature control unit with stability of ±0.1 K.

Depolarized dynamic light scattering (DDLS) was used to characterize the reorientational structural dynamics of these ILs at temperatures ranging from 185–250 K, corresponding to

structural α relaxation times of 10^{-7} through 100 s. These measurements were performed using photon correlation spectroscopy (PCS) in right angle geometry, with laser wavelength λ = 647 nm and laser power p = 200 mW. A vertically polarized beam was focused onto the sample mounted in an Oxford Optistat cryostat, and horizontally polarized scattering light was collected with a single-mode optical fiber, split between two avalanche photodiode detectors, and cross-correlated using the ALV-7004/FAST multitau digital correlator. The temperature of the sample was maintained with a stability of ±0.1 K.

RESULTS AND DISCUSSION

The complex dielectric function $\varepsilon^*(\omega) = \frac{1}{i\omega\varepsilon_0}\sigma^*(\omega)$ was measured in order to characterize both the microscopic molecular motions as well as the long-range ionic conductivity in these ILs. The real part of complex conductivity $\sigma'(\omega)$ and permittivity $\varepsilon'(\omega)$ are presented in Fig. 2 at selected temperatures for both [N2228][NTF_2] and [P2228][NTF_2]. At first glance, the [N2228][NTF_2] and [P2228][NTF_2] dielectric spectra share many qualitative similarities and also seem to closely resemble those of many other [NTF_2]-based ILs.[5, 12, 13] However, in addition to the characteristic ionic relaxation process—which is connected to the translational hopping-motion of ions in a disordered medium[14, 15] and comprises a majority of the step in $\varepsilon'(\omega)$—there are two additional relaxation features in the spectra of both ILs that clearly distinguish them from other [NTF_2]-based ILs.

At relatively low temperatures close to T_g, well-defined secondary relaxations are observed in the dielectric spectra of both ILs. These relaxations can be seen as very weak and broad steps in the real permittivity spectra recorded at relatively low temperatures (Fig. 2(b,d)). While secondary relaxations are common dynamical features of many supercooled liquids,[16-18] it was recently

demonstrated that the complex dielectric permittivity spectrum of a similar IL, 1-butyl-3-methylimidazolium bis(trifluoromethylsulfonyl)imide [BMIM][NTF_2], exhibits no visible secondary relaxations at any measured temperatures.[12] Considering that the primary differences between [BMIM][NTF_2] and these quaternary ILs are the cation variation and the presence of long alkyl side chains, the secondary β relaxations observed in these [N2228] and [P2228]-based ILs are likely related to local fluctuations of the alkyl groups. This dynamical scenario is reminiscent of the well-studied poly(n-alkylacrylates) which also exhibit pronounced secondary relaxations (the so-called "polyethylene process") that reflect local fluctuations of the alkyl side chains.[19-21]

Another unique feature in the dielectric spectra of both ILs is the presence of well-defined, slow relaxation processes which appear in $\varepsilon'(\omega)$ as additional small steps superimposed on the main ionic relaxation processes. The resulting two-step frequency dependence of the real permittivity spectrum of both [N2228][NTF_2] and [P2228][NTF_2] is readily observed at higher temperatures (Fig. 2(b,d)). The prominence and visibility of this relaxation feature is highly unusual, and to our knowledge such two-step permittivity spectra have not been observed so distinctly in other neat room temperature ionic liquids.[22, 23]

Having identified three distinct relaxations in the dielectric spectra of these ILs, we have used a fitting model to extract the dc conductivity σ_0 and the characteristic relaxation times τ_e, τ_1, and τ_2 associated with the three relaxation processes, such that

$$i\omega\varepsilon_0\varepsilon^*(\omega) = \sigma^*(\omega) = \sigma_0\left(\frac{i\omega\tau_e}{\ln(1+i\omega\tau_e)}\right) + i\omega\varepsilon_0\left(\varepsilon_\infty + \frac{\Delta\varepsilon_1}{1+(i\omega\tau_1)^{\alpha_1}} + \frac{\Delta\varepsilon_2}{1+(i\omega\tau_2)^{\alpha_2}}\right) \quad (1)$$

This first term in Eq. 1 is the approximate analytical solution of the Random Barrier Model (RBM) contribution to the complex dielectric function, which accounts for the characteristic ionic relaxation process.[14] The RBM, which considers charge transport as occurring via an ion-hopping process in a disordered matrix, has been shown to accurately describe the dielectric spectra of

many room temperature ionic liquids.[24, 25] The second term in Eq. 1 is a superposition of two Cole-Cole (CC) relaxations[26] and is included to account for the secondary β relaxation as well as the superimposed slow process. Using Eq. 1, we have fit the dielectric spectra of both [N2228][NTF_2] and [P2228][NTF_2] at all measured temperatures in the range of 185–300 K, and representative fits are shown in Fig. 2. The CC parameter of the fast β relaxation processes in both ILs were found to be highly stretched ($\alpha \approx 0.25$) at all measurement temperatures, while the CC parameter of the slow relaxation processes were nearly Debye-like ($\alpha \approx 0.90$) at all measurement temperatures.

We have calculated the ε' derivative spectrum ($\varepsilon'_{der.} = -\frac{\pi}{2} d\varepsilon'/d(\ln f)$) for both [N2228][$NTF_2$] and [P2228][$NTF_2$] to more clearly demonstrate the presence of the slow relaxation feature and better understand its nature. Figure 3 presents the derivative spectra for both ILs, which have been normalized to the peak position/amplitude of the ionic relaxation process. As is seen in Fig. 3, two relaxation peaks are clearly present in the spectra of both ILs at higher measurement temperatures. Interestingly, the dielectric strength of the slow relaxation process decreases as T_g is approached in both ILs, and eventually the process becomes indistinguishable from the primary ionic relaxation.

In addition to the peculiar temperature dependence of the dielectric strength, the peak position of this slow process appears to have a different temperature dependence than the primary ionic relaxation, becoming closer in frequency to the primary peak as the temperature decreases toward T_g. If the slow process was the sole signature of Maxwell-Wagner-Sillars (MWS) polarization, the temperature dependence of the characteristic relaxation time should closely follow that of the ionic relaxation time and dc conductivity,[27] as was recently found for a similar IL [N8881][NTF_2].[5] A strongly temperature dependent static dielectric constant could alternatively lead to the unusual temperature dependence of the observed slow relaxation times. As is seen in

Fig. 2, however, the static dielectric constant (plateau in ε') is essentially temperature independent for both ILs. As such, it is not likely that the underlying physical nature of this slow process is solely connected to MWS polarization.

Alternatively, we speculate that this slow relaxation process could instead reflect the collective reorientational dynamics of counter-ion solvation structures. In these ILs, anions have a higher probability of being excluded from the volume occupied by the long octyl group in the vicinity of the cation charge center, and thus they preferentially reside near the ethyl-rich sides of the cation charge center.[10] As a result of this high degree of counter-ion solvation anisotropy—which is not realized for many imidazolium based ILs[28] or more symmetrically decorated quaternary ammonium/phosphonium ILs[29]—a solvated ion could potentially exist in a charge neutral local environment which still has a modest dipole moment along the average direction of the long octyl side-chain. As the temperature of the liquid increases and more thermal energy is available for the octyl side-chain to fluctuate, the volume swept out by the octyl side-chain increases and effectively excludes the anions from an increasingly larger region around the cation charge center. The effect of increasing temperature consequently results in more anisotropy of the counter-ion solvation structures, causing these structures to possess larger dipole moments (and larger dielectric relaxation amplitudes).

Kashyap *et al.*[30] and Hettige *et al.*[31] recently investigated the temperature dependent structure of a similar IL [P666,14][NTF_2] in which one alkyl side chain is substantially longer than the other three. They observed anomalous temperature dependence of the X-ray scattering feature at ≈ 0.3 nm^{-1} which is associated with nanometer scale organization of polar-apolar structural motifs. In their studies, this scattering feature unexpectedly increased in intensity with increasing temperature, which was attributed to better organization of polar domains at the expense of the

organization of apolar domains. Our dielectric data correlate well to these recent structural studies, and furthermore, our proposed hypothetical physical picture describing our dielectric measurements is directly in line with these recent studies of [P666,14][NTF_2].

We have also performed depolarized dynamic light scattering (DDLS) measurements in order to characterize the reorientational structural dynamics of [N2228][NTF_2] and [P2228][NTF_2] over a similar range of temperatures as BDS. The normalized intensity correlation functions (ICF) recorded at several temperatures in the supercooled liquid regime of [N2228][NTF_2] and [P2228][NTF_2] are shown in Fig. 4. It is immediately evident from a visual inspection of these data that the decay of the ICF for both ILs occurs as a two-step process. Furthermore, the faster of the two relaxation processes appears to change significantly (relative to the main relaxation) in both time-scale and temperature dependence upon substitution of nitrogen by phosphorus in the cation charge center.

In order to extract the characteristic DDLS relaxation times, the correlation functions shown in Fig. 4 were fit with a superposition of two Kohlrausch-William-Watts (KWW) stretched exponential functions,[32] such that

$$g^2(t) - 1 = \gamma |g^1(t)|^2 = \gamma \left| a_1 \exp\left(-\left(\frac{t}{\tau_1}\right)^{\beta_1}\right) + a_2 \exp\left(-\left(\frac{t}{\tau_2}\right)^{\beta_2}\right)\right|^2 \quad (2)$$

where γ is the coherence factor of the optical system, a_1 and a_2 are the relative relaxation strengths, τ_1 and τ_2 are the characteristic relaxation times, and β_1 and β_2 are the non-exponentiality (KWW) parameters of the faster (1) and slower (2) decay processes, respectively.[33] Figure 4 depicts the fitting of Eq. 2 to the normalized intensity correlation function $g^2(t) - 1$ and the normalized field correlation function $g^1(t)$ at one representative temperature for both [N2228][NTF_2] and [P2228][NTF_2]. The characteristic DDLS relaxation times determined from the fitting are shown in Fig. 5 for both ILs, along with the corresponding characteristic BDS relaxation times.

Interestingly, the stretching parameters of the corresponding fast and slow relaxation processes were found to be nearly equivalent and temperature independent for both ILs, with β_{fast} = 0.3±0.05 and $\beta_{slow} \approx$ 0.42±0.02 in the measured temperature window.

The slow relaxation times measured via DDLS are nearly identical to the characteristic ionic relaxation times measured via BDS, although a modest decoupling of these timescales occurs near T_g as was found in recent studies of imidazolium based ILs.[12, 23, 34] These relaxation times were fit using the Vogel-Fulcher-Tammann (VFT) equation $\tau = \tau_0 \exp(\frac{A}{T-T_0})$, where τ_0, A, and T_0 are fit parameters.[35, 36] The dynamic glass transition temperature (conventionally taken as the temperature at which τ = 100 s) of each IL was determined by extrapolating the VFT fits, and it was found that $T_{g\text{-dynamic}}$ = 193 K for [N2228][NTF_2] and $T_{g\text{-dynamic}}$ = 185 K for [P2228][NTF_2]. These dynamic glass transition temperatures agree very well with the calorimetric glass transition temperatures measured via DSC (T_g = 193 K for [N2228][NTF_2] and T_g = 186 K [P2228][NTF_2]), and as such we assign the slow DDLS relaxation times to fluctuations of the cation and anion charge centers (structural α relaxation). We have also calculated the dynamic fragility $m = \left.\frac{dlog_{10}(\tau)}{d\frac{T_g}{T}}\right|_{T=T_g}$ by extrapolating these VFT fits to τ = 100 s and found these ILs to exhibit relatively fragile dynamics, where m = 71 for [N2228][NTF_2] and m = 82 for [P2228][NTF_2].[37] We speculate that the slightly larger cationic size of the phosphonium IL leads to more frustrated molecular packing, which is hypothesized to increase the dynamic fragility of supercooled liquids.[38, 39]

The fast relaxation times measured via DDLS are also seen in Fig. 5 to correspond very well with the secondary relaxation times measured via BDS for both ILs. We attribute this fast relaxation mode of both ILs to local fluctuations of the long alkyl groups of these ILs, as the slow relaxation process was previously connected to the reorientational motion of cation/anion charge

centers. The secondary relaxation of [P2228][NTF_2] has the usual characteristics of β relaxation in supercooled liquids. Not only is it many orders of magnitude faster than the structural α relaxation process near T_g, but it also has the expected Arrhenius temperature dependence $\tau = \tau_0 \exp(\frac{E_A}{kT})$ with an activation energy E_A = 55kJ/mol ≈ $36k_BT_g$ and a dynamic fragility $m \approx 16$ (at the calorimetric T_g).[40] This activation energy corresponds roughly to the combined activation energy of three collective trans-gauche transitions of the alkyl tail.[41]

The secondary relaxation process of [N2228][NTF_2], while still much faster than the α relaxation, surprisingly exhibits a mildly non-Arrhenius temperature dependence. This process in [N2228][NTF_2] is also seen to be much slower (relative to the α relaxation) than that of [P2228][NTF_2] at all measured temperatures. By fitting these relaxation times to the VFT equation, the dynamic fragility of the secondary relaxation process (at the calorimetric T_g) was found to be $m \approx 26$. These two unusual experimental facts indicate that the observed secondary relaxation process of [N2228][NTF_2] and the underlying molecular motions exhibit a mild degree of cooperativity.[42, 43]

While the presence of a weakly non-Arrhenius secondary relaxation process in the reorientational dynamics of [N2228][NTF_2] is certainly unusual, it is not entirely unexpected. The dynamics of the widely studied poly(n-alkylacrylate) based polymers have been shown to exhibit pronounced secondary relaxations in addition to the structural α relaxation.[19] As the side chain length n of these polymers increases, the secondary relaxation changes from a purely Arrhenius type of temperature dependence at n = 4 to more VFT like with increasing alkyl chain length up to n = 8 carbon atoms. This secondary relaxation process was identified as being associated with the fluctuations of alkyl moieties in nanophase segregated, alkyl-rich domains of the polymer

matrix. As the alkyl chains increase in length, the alkyl domain size grows, and the degree of cooperativity of the alkyl unit dynamics correspondingly becomes greater.

It has been shown by both structural and dynamical studies that quaternary ammonium and phosphonium based ILs exhibit nanophase segregation of the charge-rich ion-centers from the apolar alkyl sidechains—similar to what is observed in the poly(n-alkylacrylate) based polymers.[44] In analogy to these studies, our results on the dynamics in these ILs suggest that the alkyl-rich nanodomains of [N2228][NTF_2] are slightly larger and more well-defined than the corresponding nanostructures of [P2228][NTF_2]. We have recently shown that for [N8881][NTF_2], nanometer scale, long-lived supramolecular aggregates form in the liquid matrix,[5] and it would be very interesting to see how the alkyl chain length and mole fraction of alkyl groups effects the formation of aggregate structures. Furthermore, it would be very interesting to see if the homologous IL [P8881][NTF_2] exhibits the dynamical signature of supramolecular aggregate nanostructures. Further studies are being pursued to investigate these questions.

While these experimental data exhibit trends similar to the dynamics of the poly(n-alkylacrylates), which indicates some degree of nanoscale organization of alkyl rich domains occurs in these ILs, the unusual differences upon atomic substitution of nitrogen ([N2228][NTF_2]) with phosphorus ([P2228][NTF_2]) has at this point not been resolved. Recently, Lee *et al*. performed 2D NMR experiments on the same ILs studied herein in order to understand how counter-ion interactions differ depending on the atomic identity of the cation center, i.e. $[N2228]^+$ versus $[P2228]^+$.[11] In this study, the authors found that the $[NTF_2]^-$ anions in [N2228][NTF_2] interact primarily with the cation charge center and only weakly interact with the octyl side chain. Conversely, the $[NTF_2]^-$ anions in [P2228][NTF_2] were found to interact much more strongly with the octyl side chain. These differences in inter-ionic interactions provide a strong foundation to

interpret our observed experimental dynamical data. Since the anions interact and coordinate much more readily with the cation charge center of [N2228][NTF_2] when compared to [P2228][NTF_2], more well-defined exclusion of the anions from the alkyl-rich nanodomains of [N2228][NTF_2] occurs. This difference in nanoscale structure fits well within the framework of the Hard and Soft Acids and Bases (HSAB) concept, which predicts that the "harder" ammonium cation charge center should more readily coordinate with the $[NTF_2]^-$ counterion when compared to its ammonium homolog.[45-47] As a direct consequence of these differences in inter-ionic interactions and nanoscale structural organization, the alkyl domains of [N2228][NTF_2] exhibit significantly different (and mildly cooperative) relaxation dynamics when compared to [P2228][NTF_2].

Not only do weaker interionic interactions disrupt the formation of cohesive alkyl domains in [P2228][NTF_2], but they also contribute to a strong reduction in electrostatic friction between ions and concomitantly reduce the glass transition temperature. As seen in Fig. 6, the dc ionic conductivity of [P2228][NTF_2] is significantly greater than that of [N2228][NTF_2] at all measured temperatures, which has been observed previously when comparing the conductivity of ammonium and phosphonium based ILs.[7, 47] As shown in the inset of Fig. 6, this enhancement is primarily due to the lower glass transition temperature of [P2228][NTF_2] relative to [N2228][NTF_2].

CONCLUSION

The ionic conductivity and reorientational structural dynamics in a homologous pair of ammonium [N2228][NTF_2] and phosphonium [P2228][NTF_2] based room temperature ionic liquids was studied in a broad temperature range using broadband dielectric spectroscopy and depolarized dynamic light scattering. We have found that the chemical identity of the cation center atom has a

pronounced effect on both long-range ion conduction as well as structural α relaxation in these quaternary ILs. The calorimetric glass transition temperature of [P2228][NTF_2] (T_g = 186 K) was found to be moderately lower than that of [N2228][NTF_2] (T_g = 193 K) upon substitution of the cation center atom. As a consequence of the increased molecular mobility—which is attributed to weaker interactions between anions and the cation charge centers—the phosphonium based IL exhibits significantly higher ionic conductivity at all studied temperatures.

Additionally, pronounced secondary relaxation processes were observed in the DDLS spectra of these ILs, and these relaxations were also found to exhibit unexpected differences. Relative to the structural α relaxation, the secondary relaxation process of [N2228][NTF_2] was found to be several orders of magnitude slower than the secondary relaxation process of [P2228][NTF_2] at all measured temperatures. While this process in [P2228][NTF_2] exhibited an Arrhenius type of temperature dependence—characteristic of local β relaxations—the secondary relaxation in [N2228][NTF_2] was found to exhibit a weakly non-Arrhenius type of thermal activation. This unusual finding indicates that the secondary relaxation process of [N2228][NTF_2] is mildly cooperative in nature. We suggest that these differences may also be attributed to the way in which counter-ion coordination occurs in these structurally homologous ILs. The weaker interaction and coordination between the anions and cation charge centers necessarily leads to less well defined nanoscale segregation of the hydrophobic alkyl moieties, which consequently inhibits cooperative relaxation dynamics in the alkyl-rich regions of phosphonium based ILs.

ACKNOWLEDGEMENT

This work was funded by the NSF chemistry program through grant no. CHE-1213444. J.R.S. thanks the UT/ORNL Science Alliance for support through the JDRD Collaborative Cohort Program.

REFERENCES

1. J. Sun, D. MacFarlane and M. Forsyth, Ionics **3**, 356 (1997).

2. J. Sun, M. Forsyth, and D. MacFarlane, J. Phys. Chem. B **102**, 8858 (1998).

3. D. McFarlane, J. Sun, J. Golding, P. Meakin, and M. Forsyth, Electrochim. Acta **45**, 1271 (2000).

4. W. Xu, E. I. Cooper, and C. A. Angell, J. Phys. Chem. B **107**, 6170 (2003).

5. P. J. Griffin, A. P. Holt, Y. Wang, V. N. Novikov, J. R. Sangoro, F. Kremer, and A. P. Sokolov, J. Phys. Chem. B **118**, 783 (2014).

6. K. Shimizu, A. l. A. Pádua, and J. N. Canongia Lopes, J. Phys. Chem. B **114**, 15635 (2010).

7. K. Tsunashima and M. Sugiya, Electrochem. Commun. **9**, 2353 (2007).

8. H. Shirota, H. Fukazawa, T. Fujisawa, and J. F. Wishart, J. Phys. Chem. B **114**, 9400 (2010).

9. P. J. Carvalho, S. P. Ventura, M. L. Batista, B. Schröder, F. Gonçalves, J. Esperança, F. Mutelet, and J. A. Coutinho, J. Chem. Phys. **140**, 064505 (2014).

10. H. K. Kashyap, C. S. Santos, R. P. Daly, J. J. Hettige, N. S. Murthy, H. Shirota, E. W. Castner Jr, and C. J. Margulis, J. Phys. Chem. B **117**, 1130 (2013).

11. H. Y. Lee, H. Shirota, and E. W. Castner Jr, J. Phys. Chem. Lett. **4**, 1477 (2013).

12. P. Griffin, A. L. Agapov, A. Kisliuk, X.-G. Sun, S. Dai, V. N. Novikov and A. P. Sokolov, J. Chem. Phys. **135**, 114509 (2011).

13. J. Sangoro, C. Iacob, S. Naumov, R. Valiullin, H. Rexhausen, J. Hunger, R. Buchner, V. Strehmel, J. Kärger, and F. Kremer, Soft Matter **7**, 1678 (2011).

14. J. C. Dyre, J. Appl. Phys. **64**, 2456 (1988).

15. J. C. Dyre and T. B. Schrøder, Rev. Mod. Phys. **72**, 873 (2000).

16. A. Kudlik, C. Tschirwitz, S. Benkhof, T. Blochowicz, and E. Rössler, Europhys. Lett. **40**, 649 (1997).

17. A. Kudlik, C. Tschirwitz, T. Blochowicz, S. Benkhof, and E. Rössler, J. Non-Cryst. Solids **235**, 406-411 (1998).

18. K. Ngai and M. Paluch, J. Chem. Phys. **120**, 857 (2004).

19. M. Beiner and H. Huth, Nat. Mater. **2**, 595 (2003).

20. A. Arbe, A.-C. Genix, J. Colmenero, D. Richter, and P. Fouquet, Soft Matter **4**, 1792 (2008).

21. K. Ngai and M. Beiner, Macromolecules **37**, 8123 (2004).

22. J. Sangoro, C. Iacob, A. Serghei, S. Naumov, P. Galvosas, J. Kärger, C. Wespe, F. Bordusa, A. Stoppa, J. Hunger, R. Buchner, and F. Kremer, J. Chem. Phys. **128**, 214509 (2008).

23. P. J. Griffin, A. L. Agapov, and A. P. Sokolov, Phys. Rev. E **86**, 021508 (2012).

24. J. R. Sangoro, Colloid and Polym. Sci. **292** (8), 1933-1938 (2014).

25. J. R. Sangoro and F. Kremer, Accounts Chem Res. **45** (4), 525-532 (2011).

26. K. S. Cole and R. H. Cole, J. Chem. Phys. **9**, 341 (1941).

27. F. Kremer and A. Schönhals, *Broadband Dielectric Spectroscopy*. (Springer, Berlin, 2003).

28. H. V. Annapureddy, H. K. Kashyap, P. M. De Biase, and C. J. Margulis, J. Phys. Chem. B **114**, 16838 (2010).

29. C. S. Santos, H. V. Annapureddy, N. S. Murthy, H. K. Kashyap, E. W. Castner Jr, and C. J. Margulis, J. Chem. Phys. **134**, 064501 (2011).

30. H. K. Kashyap, C. S. Santos, H. V. Annapureddy, N. S. Murthy, C. J. Margulis, and E. W. Castner Jr, Faraday Discuss. **154**, 133 (2012).

31. J. J. Hettige, H. K. Kashyap, and C. J. Margulis, J. Chem. Phys. **140**, 111102 (2014).

32. G. Williams and D. C. Watts, T. Faraday Soc. **66**, 80 (1970).

33. B. J. Berne and R. Pecora, *Dynamic Light Scattering: With Applications to Chemistry, Biology, and Physics* (Dover, New York, 1976).

34. N. Ito and R. Richert, J. Phys. Chem. B **111**, 5016 (2007).

35. H. Vogel, Phys. Z **22**, 645 (1921).

36. G. S. Fulcher, J. Am. Ceram. Soc. **8**, 339 (1925).

37. R. Böhmer, K. Ngai, C. Angell, and D. Plazek, J. Chem. Phys. **99**, 4201 (1993).

38. J. Dudowicz, K. F. Freed, and J. F. Douglas, J. Chem. Phys. **124**, 064901 (2006).

39. W.-S. Xu and K. F. Freed, Macromolecules **47**, 6990 (2014).

40. K. L. Ngai, *Relaxation and Diffusion in Complex Systems* (Springer, New York, 2011).

41. K. B. Wiberg and M. A. Murcko, J. Am. Chem. Soc. **110**, 8029 (1988).

42. G. Adam and J. H. Gibbs, J. Chem. Phys. **43**, 139 (1965).

43. R. Richert and C. Angell, J. Chem. Phys. **108**, 9016 (1998).

44. A. Triolo, O. Russina, R. Caminiti, H. Shirota, H. Y. Lee, C. S. Santos, N. S. Murthy, and E. W. Castner Jr, Chem. Comm. **48**, 4959 (2012).

45. R. G. Pearson, J. Am. Chem. Soc. **85**, 3533 (1963).

46. A. Tsurumaki, J. Kagimoto, H. Ohno, Polym. Adv. Technol. **22**, 1223 (2011).

47. S. Seki, K. Hayamizu, S. Tsuzuki, K. Fujii, Y. Umebayashi, T. Mitsugi, T. Kobayashi, Y. Ohno, Y. Kobayashi, Y. Mita, H. Miyashiro, and S.-I. Ishiguro, Phys. Chem. Chem. Phys. **11**, 3509 (2009).

FIGURE 1.

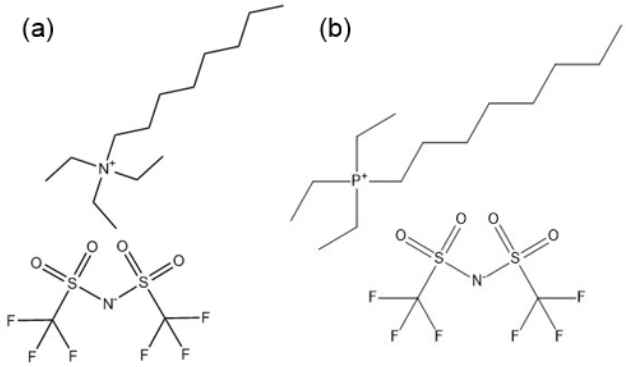

FIGURE 1 CAPTION.

Chemical structures of (a) octyltriethylammonium bis(trifluoromethylsulfonyl)imide ([N2228][NTF_2]) and (b) octyltriethylphosphonium bis(trifluoromethylsulfonyl)imide ([P2228][NTF_2]).

FIGURE 2.

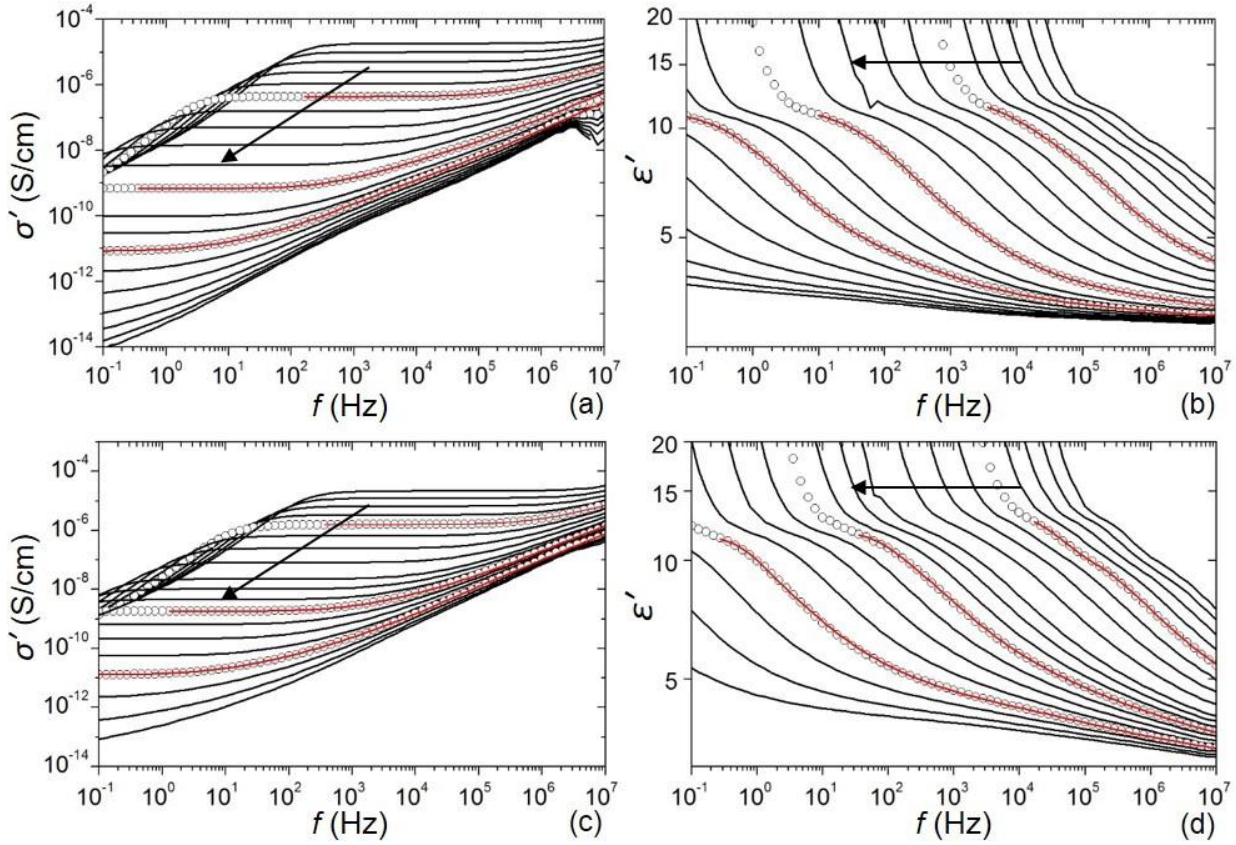

FIGURE 2 CAPTION.

The real part of the complex conductivity σ' and permittivity ε' spectrum is shown for [N2228][NTF_2] (a and b, respectively) and for [P2228][NTF_2] (c and d, respectively) at select temperatures ([N2228][NTF_2]: 185–210 K in 2.5 K steps, 210–260 K in 5 K steps; [P2228][NTF_2]: 185–210 K in 2.5 K steps, 210–250 K in 5 K steps). The red solid lines are fits of the experimental data recorded at select temperatures (open circles) using Eq. 1, and the solid arrows indicate the direction of decreasing temperature.

FIGURE 3.

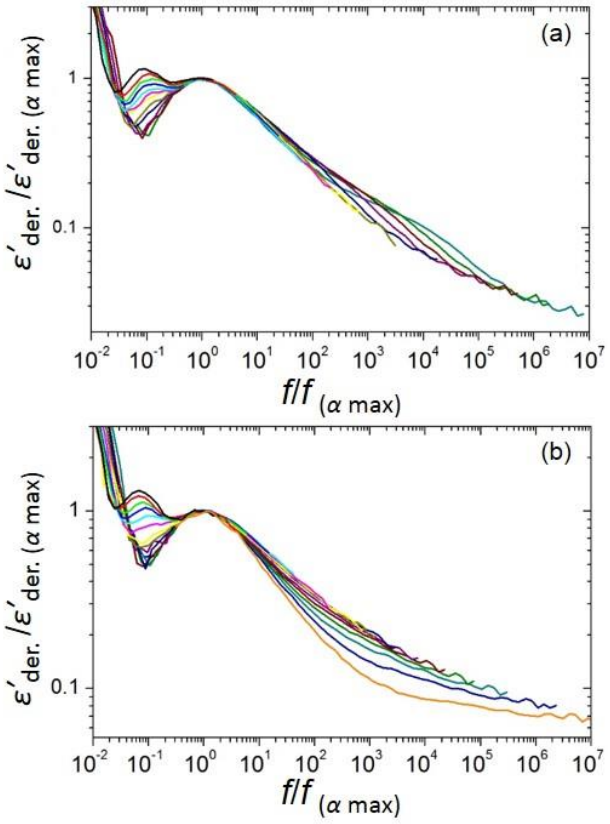

FIGURE 3 CAPTION.

The calculated ε' derivative spectra ($\varepsilon'_{der.} = -\frac{\pi}{2} d\varepsilon'/d(\ln f)$) are shown for (a) [N2228][NTF_2] in the temperature range 197.5–250 K and (b) [P2228][NTF_2] in the temperature range 190–240 K. The spectra have been normalized to the apparent ionic relaxation peak position and amplitude. A well pronounced slow relaxation process is clearly observed in the spectra of both ILs that decreases in amplitude and becomes closer in timescale to the ionic relaxation as T_g is approached.

FIGURE 4.

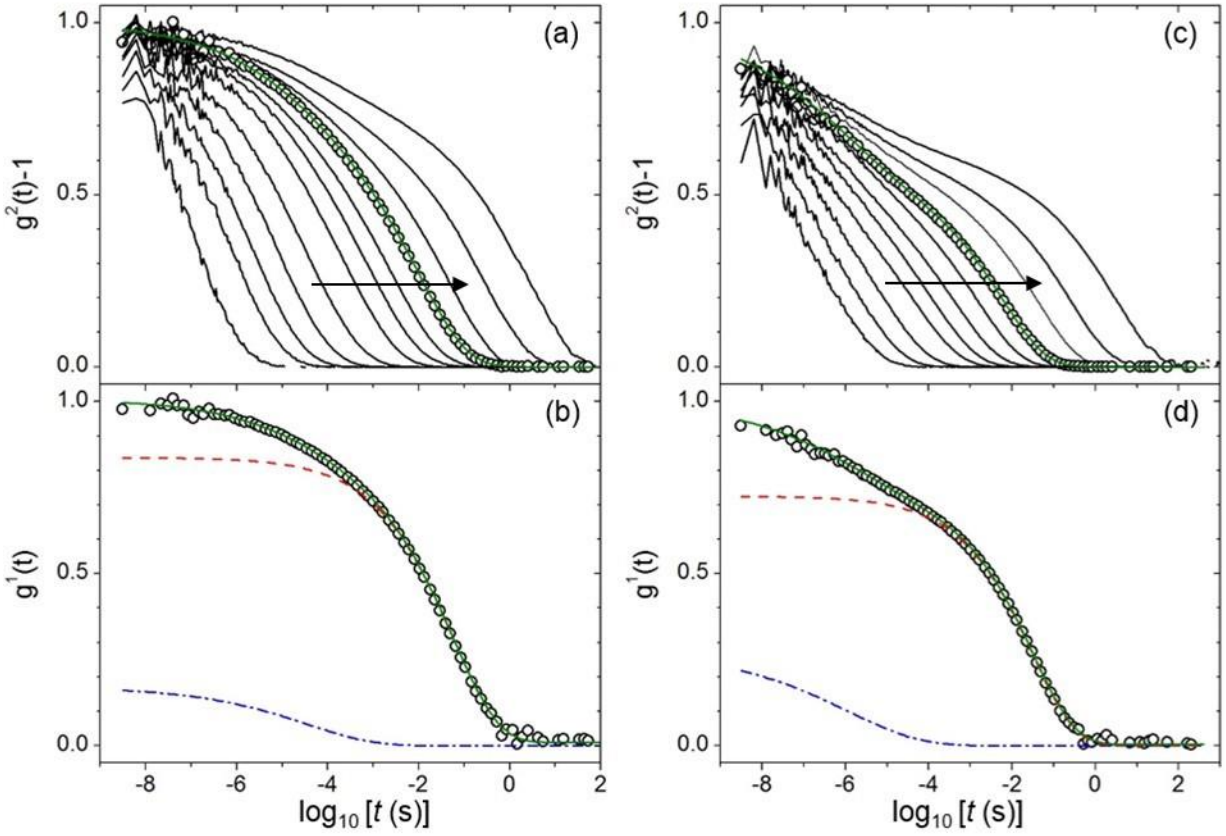

FIGURE 4 CAPTION.

Normalized intensity correlation functions $g^2(t) - 1$ (ICF) plotted at select temperatures for (a) [N2228][NTF_2] (195–210 K in 2.5 K steps, 210–230 K in 5 K steps, 240 K) and (c) [P2228][NTF_2] (187.5–205 K in 2.5 K steps, 205–220 K in 5 K steps). Solid arrows indicate the direction of decreasing temperature. The green solid lines are the fits of Eq. 2 to the normalized ICFs (open circles) recorded at 202.5 K ([N2228][NTF_2]) and 195 K ([P2228][NTF_2]). Corresponding normalized field correlation functions $g^1(t)$ (FCF) are shown measured at 202.5 K for (b) [N2228][NTF_2] and at 195 K for (d) [P2228][NTF_2]. The red dashed line represents the contribution to the total FCF from the structural α relaxation, the blue dash-dotted line represents to contribution from the secondary relaxation, and the green solid line is the total fit using Eq. 2.

FIGURE 5.

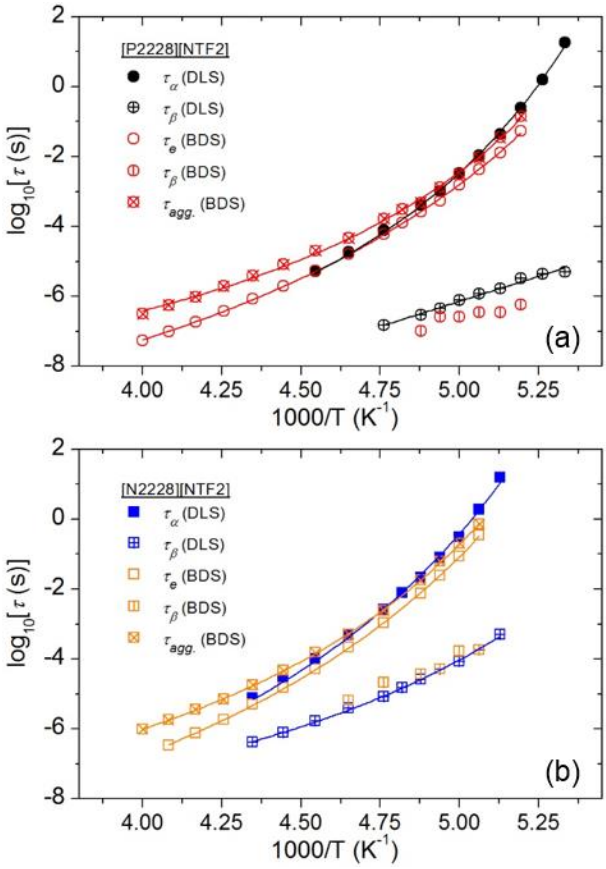

FIGURE 5 CAPTION.

Characteristic timescales of structural relaxation and charge transport measured via depolarized dynamic light scattering and broadband dielectric spectroscopy are shown plotted against inverse temperature for (a) [P2228][NTF_2] and (b) [N2228][NTF_2]. The relaxation times τ_e and $\tau_{agg.}$ denote the characteristic timescales of the ionic relaxation process and the slow, aggregate relaxation process observed in the dielectric spectra of these ILs, respectively. The solid lines are fits to the data using the Vogel-Fulcher-Tammann (VFT) equation, while the secondary relaxation of [P2228][NTF_2] is fit using the Arrhenius equation.

FIGURE 6.

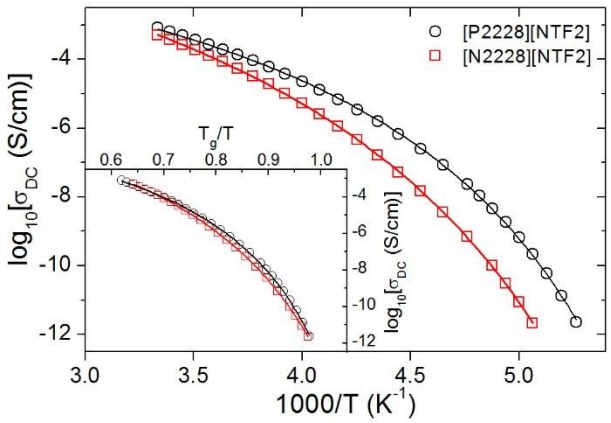

FIGURE 6 CAPTION.

The ionic (dc) conductivity of [N2228][NTF_2] and [P2228][NTF_2] is shown plotted against inverse temperature in the main pane, as well as against T_g-scaled inverse temperature in the inset. The solid lines are Vogel-Fulcher-Tammann fits to the data (open symbols).